The Influence of Source Location on the Structural-Acoustic Interaction of Cylinders

J. J. Kelly*
Old Dominion University, Norfolk, Virginia
and
C. R. Fuller†
Virginia Polytechnic Institute and State University, Blacksburg, Virginia

This paper deals with the response of an infinite elastic cylinder to simple exterior acoustic sources (monopole and dipole). A coupled solution involving spectral equations of motion is used to evaluate the parameters of interior pressure, power flow into the cylinder, and variation of acoustic intensity with angular position at the cylinder wall. The variation of these parameters with source characteristic and location as well as observation point is investigated in order to uncover the nature of the interaction phenomena. In general, the interior pressure was found to fall quickly for an initial increase in source location and then more slowly. Dipole sources were also found to excite far lower interior sound levels than monopoles. The results are of use in leading to an understanding of the interaction of propeller acoustic sources with aircraft fuselages.

Nomenclature

a = shell mean radius
C_f, C_L = fluid free and shell free speeds of propagation, respectively
d = dipole source separation
FL = fluid loading term
f_n = pressure forcing term
h = shell wall thickness
H_n = Hankel function of first kind
I = radial intensity
I_{33} = (3,3) element of inverse matrix
J_n = Bessel function
k = free acoustic wavenumber
k_r, k_n = radial and axial wavenumbers, respectively
K_p, K_w = pressure and shell response integrands, respectively
L = shell response matrix
n = circumferential mode number
p_{ex}, p_i = acoustic pressure of external and interior fields, respectively.
p_{inc}, p_s = acoustic pressure of incident and scattered fields, respectively
p_0 = pressure amplitude of monopole source
p^{nd}, P^{nd} = nondimensional acoustic pressure and line power, respectively
P = acoustic line power
r, θ, x = cylindrical coordinate
r_i = radial location of monopole source
R = nondimensional radial location
R_s = source nondimensional location
t = time
w = shell radial displacement vector
$\tilde{U}, \tilde{V}, \tilde{W}$ = shell spectral displacement amplitudes
X = nondimensional axial location
Y_n = column vector of shell displacements
β = shell thickness parameter
ϵ_n = 1 if $n=0$, = 2 if $n>0$
ρ_f, ρ_s = density of fluid field and shell material, respectively
Ω = nondimensional source frequency
ν = Poisson's ratio
ω = source frequency (rad/s)

Superscripts and Subscripts

$( )^*$ = complex conjugate
i = source index number

Received Feb. 18, 1985; revision received Aug. 9, 1985.

*Assistant Professor, Mechanical Engineering and Mechanics. Member AIAA.
†Associate Professor, Mechanical Engineering.

Introduction

THERE has been increased interest in advanced turboprop design (ATP), due to the present demand for efficient aircraft. A disadvantage of ATPs is the high radiated acoustic levels due to supersonic tip speeds, and there is some concern that cabin levels may exceed acceptable criteria.[1] Hence, there has been a renewed interest in investigating aspects of interior noise.[2] However, there remains much work to be done, particularly in understanding the fundamental mechanisms by which sound transmits into the aircraft fuselage.

In this investigation, the effect of source location on the response of a fluid-filled infinite cylindrical shell excited by an exterior monopole or dipole acoustic source is studied. The problem considered is related to the interaction of propeller-radiated sound with aircraft fuselages. An analysis developed by Fuller[3] was modified for this investigation. The analysis uses spectral equations of motion to describe the source radiation, shell response, and contained acoustic field vibration. The formulation allows a coupled solution of motion to be obtained for a prescribed source. Two sources, a monopole and a dipole, are considered. The dipole source is constructed as a superposition of two monopoles with a small separation distance ($d/a=0.1$). The monopoles are located on a line perpendicular to the cylinder axis ($\theta=0$, $x=0$) to maximize the influence of source amplitude and directivity on the shell response. Due to its elasticity, the shell responds to the incident acoustic field and thus transmits energy to the interior acoustic space.

The parameters of interior acoustic pressure, radial acoustic intensity at the shell wall interior, and acoustic line power flow into the cavity are studied for a varying source location. By varying the source characteristic from a

monopole to a dipole, the influence of source directivity and radiation efficiency on the above parameters is also studied. The relevance of the results to interior noise in propeller aircraft is considered. To the authors' knowledge, the structural-acoustic coupling problem presented in this paper has not been previously studied for either a monopole or dipole source.

Problem Formulation

For the structural-acoustic coupling problem considered in this paper, the interaction of three regimes must be considered. These are the exterior pressure field (including the source term), the shell structural response, and the interior acoustic pressure field. Mathematically the coupling occurs through the kinematic condition that any particle on each surface of the shell remain on the shell surface as it oscillates. This boundary condition is transferred to the undisturbed mean radius of the shell, where it is implemented. This is accomplished by assuming a Taylor expansion for the shell thickness and small amplitudes of oscillations.

Both the exterior and interior acoustic fields are governed by the Helmholtz equation. The governing equations for the shell response can be expressed in matrix form so that the three shell displacement components are coupled. Only the shell radial displacement is needed to determine the exterior and interior acoustic fields.

The cylindrical coordinate system and geometry employed in the analysis are shown in Fig. 1. The analysis basically follows the one used in Ref. 3 and is thus presented here in concise form.

In the exterior region, the acoustic pressure can be decomposed into an incident field and a scattered field,[4] such that,

$$p_{ex} = p_{inc}(r,\theta,x) + p_s(r,\theta,x) \tag{1}$$

In Eq. (1), p_{ex} is the total acoustic pressure, p_{inc} the incident pressure due to the source, and p_s the scattered pressure due to cylinder vibration.

The governing equation for p_{ex} is

$$\nabla^2 p_{ex} + k^2 p_{ex} = \frac{-4\pi p_0 \delta(r-r_i)\delta(\theta)\delta(x)}{r} \tag{2}$$

which is the inhomogeneous Helmholtz equation in cylindrical coordinates. To complete the problem formulation, a boundary condition must be imposed at the shell surface. The proper boundary condition is continuity of particle displacement. This results in the following linearized boundary condition.

$$\left.\frac{\partial p_{ex}}{\partial r}\right|_{r=a} - \rho_f \omega^2 w(\theta,x) \tag{3}$$

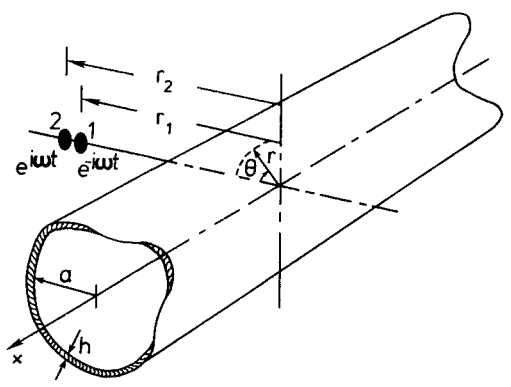

Fig. 1 Geometry and coordinate system.

The shell response in the nth circumferential mode can be written in matrix form as[3]

$$L_n Y_n = f_n \tag{4}$$

In this expression, L_n is a 3×3 matrix, the coefficients of which are given by

$$L_{11} = -\Omega^2 + (k_n a)^2 + \tfrac{1}{2}(1-\nu)n^2 \tag{5a}$$

$$L_{12} = \tfrac{1}{2}(1+\nu)n(k_n a) \tag{5b}$$

$$L_{13} = \nu(k_n a) \tag{5c}$$

$$L_{21} = L_{12} \tag{5d}$$

$$L_{22} = -\Omega^2 + \tfrac{1}{2}(1-\nu)(k_n a)^2 \tag{5e}$$

$$L_{23} = n \tag{5f}$$

$$L_{31} = L_{13} \tag{5g}$$

$$L_{32} = L_{23} \tag{5h}$$

$$L_{33} = -\Omega^2 + 1 + \beta^2[(k_n a)^2 + n^2]^2 - FL \tag{5i}$$

where the fluid loading term due to coupled fluid motion is

$$FL = \Omega^2 (h/a)^{-1}[(\rho_f/\rho_s)J_n(k_r a)/J_n'(k_r a)k_r a - (\rho_f/\rho_s)H_n(k_r a)/H_n'(k_r a)k_r a] \tag{6}$$

In Eqs. (5) and (6), Ω is a nondimensional shell frequency given by $\Omega = \omega a/C_L$, and β the shell thickness parameter given by $\beta^2 = h^2/12a^2$.

The source forcing terms for acoustic excitation due to a dipole are given by a column matrix such that

$$f_1 = 0 \tag{7a}$$

$$f_2 = 0 \tag{7b}$$

$$f_3 = (2/\sqrt{2\pi})\epsilon_n p_{01}[H_n(k_r r_1)/H_n'(k_r a)k_r a][\Omega^2/\rho_s\omega^2 h] - 2(\sqrt{2\pi})\epsilon_n p_{02}[H_n(k_r r_2)/H_n'(k_r a)k_r a][\Omega^2/\rho_s\omega^2 h] \tag{7c}$$

For monopole excitation the source amplitude p_{02} is set to zero.

The shell spectral displacements Y_n are a column matrix such that

$$Y_n = \begin{bmatrix} \bar{U}_n \\ \bar{V}_n \\ \bar{W}_n \end{bmatrix} \tag{8}$$

By inverting Eq. (4), $\bar{W}_n$ can be determined.This will then permit the calculation of the associated exterior and interior pressure fields.

The interior pressure field is governed by the homogeneous Helmholtz equation,

$$\nabla^2 p_i + k^2 p_i = 0 \tag{9}$$

Again, the appropriate boundary condition is continuity of particle displacement at the shell/fluid interface, which reduces to the following expression

$$\left.\frac{\partial p_i}{\partial r}\right|_{r=a} = \rho_f \omega^2 w(\theta,x) \tag{10}$$

With the statement of the problem complete, the solution can now be determined. Specific details of the analysis can be found in Ref. 3.

Solution

The solution of the above problem can be expressed as products of circumferential normal modes and Fourier transforms in the axial directions.[3,5] For the shell radial displacement, the solution is (for a dipole)

$$\frac{w}{p_0/a}\frac{\Omega^2}{\pi\rho_s h\omega^2}=\sum_{n=0}^{\infty}\epsilon_n\cos(n\theta)\int_{-\infty}^{\infty}K_w\left(\frac{x}{a},r_1\right)\mathrm{d}(k_n a)-\sum_{n=0}^{\infty}\epsilon_n\cos(n\theta)\int_{-\infty}^{\infty}K_w\left(\frac{x}{a},r_2\right)\mathrm{d}(k_n a) \tag{11}$$

where the displacement integrand is given by

$$K_w(x/a,r_i)=H_n(k_r r_i)/H_n'(k_r a)k_r a I_{33}\times\exp[i(k_n a)(x/a)] \tag{12}$$

In Eqs. (11) and (12) r_i is the radial location of the source ($i=1,2$), and the dipole source amplitudes have been set equal to p_0. The term I_{33} is a variable associated with inversion of matrix L. The radial wavenumber obeys

$$k_r=\frac{1}{a}\left[\Omega^2\left(\frac{C_L}{C_f}\right)^2-(k_n a)^2\right]^{1/2} \tag{13}$$

For a monopole source, only the first summation of Eq. (11) is retained.

Similarly, the interior acoustic pressure can be evaluated from

$$\frac{p_i}{(\rho_0/a)(\rho_f/\rho_s)\Omega^2(h/a)^{-1}\pi^{-1}}=\sum_{n=0}^{\infty}\epsilon_n\cos(n\theta)\int_{-\infty}^{\infty}K_p\left(\frac{x}{a},r_1,r\right)\mathrm{d}(k_n a)-\sum_{n=0}^{\infty}\epsilon_n\cos(n\theta)\int_{-\infty}^{\infty}K_p\left(\frac{x}{a},r_2,r\right)\mathrm{d}(k_n a) \tag{14}$$

where the pressure integrand is given by

$$K_p(x/a,r_1,r)=[H_n(k_r r_i)/H_n'(k_r a)k_r a]\times[J_n(k_r r)/J_n'(k_r a)k_r a]I_{33}\exp[i(k_n a)x/a] \tag{15}$$

Again, for a monopole source, only the first summation of Eq. (14) would be considered.

The calculation of the interior acoustic pressure and the shell radial displacement allows the calculation of two relevant acoustic quantities: radial acoustic intensity and power flow per unit length (line power). Both quantities are calculated at the interior of the shell wall and are evaluated from the following relationships:

$$I(x,\theta)=\tfrac{1}{2}Re[p_i(\dot{w})^*] \tag{16}$$

Integrating the intensity over the shell circumference permits the calculation of the line power P. Mathematically, this is given by

$$P=\int_0^{2\pi}I(x,\theta)a\mathrm{d}\theta \tag{17}$$

By varying r_i, the effect of source location on the above parameters can be studied. It should be noted that Eqs. (16) and (17) calculate power and intensity flow between the shell and the contained fluid.

Table 1 Material properties

Material	Young's modulus, N/m^2	Poisson's ratio	Density, kg/m^3	Free wave speed, m/s
Aluminum	7.1×10^{10}	0.33	2700	5150
Air	—	—	1.2	343

Results

The fundamental problem considered in this investigation was originally considered in order to gain some insight into how propeller noise interacts with an aircraft fuselage and transmits to the interior. Thus, it is appropriate to choose frequencies and dimensions of the system that correspond to an aircraft application. Consequently, the following results were calculated for a representative aircraft situation. The shell material was assumed to be aluminum with a nondimensional wall thickness of $h/a=.001$. The propagating medium was assumed to be air. Material properties are given in Table 1. For the results presented, the nondimensional frequency investigated was chosen to be $\Omega=0.2$. For example, this would correspond to a frequency of 150 Hz in a 2.2-m-diam fuselage. These values are considered typical of future ATP applications. The results presented in this paper were found to be generally similar for a nondimensional frequency range of $0<\Omega<0.5$.

As discussed by Mixson et al.,[6] the acoustic source due to a propeller is semicompact and can be considered to be located on a line between the fuselage center and propeller hub at approximately two-thirds the propeller disk radius. Similarly, comparisons made by Mahan and Fuller[7] show that a dipole (and a monopole) provides a reasonable approximation of propeller fuselage signatures. Thus, a typical source application location would be $r_1/a=3.0$ and $r_2=3.1$, i.e., a source of $d/a=0.1$.

The integrals of Eqs. (11) and (14) were evaluated following the method outlined in Ref. 3. The infinite sums of these equations were found to converge to sufficient accuracy for ten circumferential modes and, thus, the infinite sums were truncated at $n=9$.

Figures 2-4 depict the variation of the nondimensional interior acoustic pressure with source location. In this study, the nondimensional pressure is defined as

$$p_i^{nd}=p_i/[(p_0/a)(1/\pi)\Omega^2(\rho_f/\rho_s)(h/a)^{-1}] \tag{18}$$

Source location was expressed in nondimensional form in terms of shell radius as $R_s=r_1/a$. Similarly the radial and axial coordinates were expressed as $R=r/a$ and $X=x/a$.

Figure 2 shows the variation in internal pressure at $R=1$, $\theta=0$, and $X=0$ (source plane) with increasing dipole source location. The results of Fig. 2 show that the internal pressure falls rapidly as the source is moved from one to three shell radii away from the cylinder axis. This effect was thought to be due to the near field of the dipole source extending approximately two shell radii. By "near field" the authors mean that part of the source radiation field where interior levels fall rapidly and the radiated intensity is complex (i.e., the radiated field has a component of reactance). Although one would expect similar behavior for a free-field pressure, it should be noted that the results of Fig. 2 are for *interior* pressure and thus include the effects of the response of the shell. As shown by Fuller,[3] the internal pressure distribution is a result of the shell circumferential modal response. As only part of the exterior of the shell is immersed in the source near field, it is of interest to see that the internal pressure response also exhibits a near field type of behavior similar to the free-field radiation of the source.

The results of Fig. 3 are for a situation similar to the previous figure except that the observation point is at $R=0$

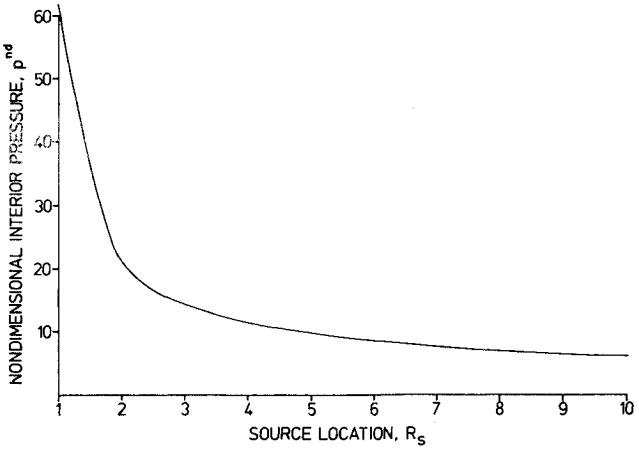

Fig. 2 Interior pressure dependence on source location, $R=1$, $X=0$, $\theta=0$, and $\Omega=0.2$ (dipole source).

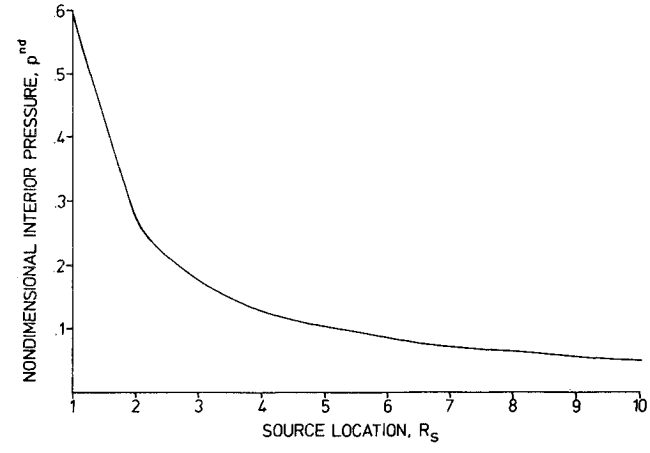

Fig. 3 Interior pressure dependence on source location, $R=0$, $X=0$, $\theta=0$, and $\Omega=0.2$ (dipole source).

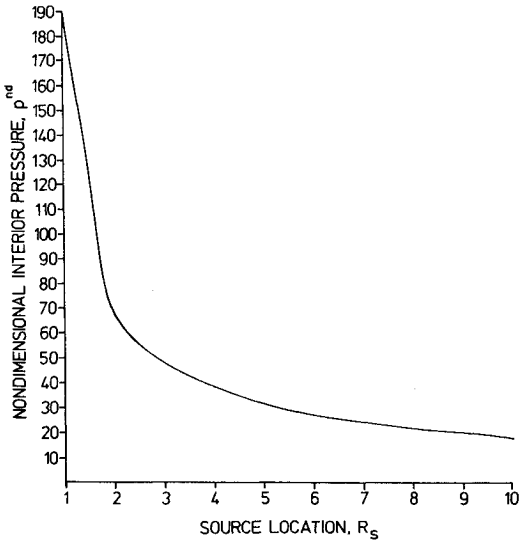

Fig. 4 Interior pressure dependence on source location, $R=1$, $X=0$, $\theta=0$, and $\Omega=0.2$ (monopole source).

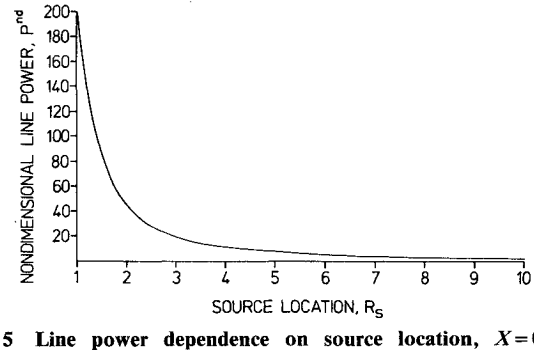

Fig. 5 Line power dependence on source location, $X=0$ and $\Omega=0.2$ (dipole source).

on the shell centerline. Again, at this observation point a similar near-field effect is exhibited by the internal pressure as the source is moved away from the shell surface. It can also be seen that the acoustic pressure is far less in magnitude at the shell centerline than at the wall, because the field at the centerline is entirely due to the $n=0$ circumferential mode, which is poorly excited by the dipole source.

When the source is replaced by a monopole, similar trends are observed as the source is moved away from the shell surface. Figure 4 presents results for a monopole source where the internal observation point is at $R=1$, $X=0$, and $\theta=0$. Again, the near field of the monopole source appears to extend approximately, two shell radii at this excitation frequency. It is also apparent that the interior levels are much greater for a monopole source than a dipole source, an effect that is undoubtably due to the higher radiation efficiency of the monopole. However, it must again be noted that the internal pressure is coupled directly to shell vibration and is thus dependent on the shell response as well as on source strength and directivity. Thus, the omnidirectional source is a more efficient radiator of sound *to the interior* of the shell for the frequency considered. Generally, results similar to those presented in Figs. 2-4 were found at other locations inside the shell.

Also of interest is the total acoustic energy flowing into the shell interior. The line acoustic power was evaluated using Eq. (17) and is plotted in nondimensional form such that

$$P^{nd} = -P/[(\tfrac{1}{2}\pi)(p_0/a)^2\Omega^4(\rho_f/\rho_s)(h/a)^{-2}\omega^{-1}\rho_s^{-1}] \quad (19)$$

for various source locations. It should be noted that due to the convention assumed for shell vibration, a negative absolute power flow corresponds to an inward power flow. Line power vs source position is plotted in Fig. 5, where the observation point is at $X=0$ and the source is a dipole. In Fig. 5, one can again see the near-field effect of the source on line power for source locations $1 \lesssim R_s \lesssim 3$. Also, note that for this case, where the calculations are performed in the source plane $X=0$, the power flow is from the shell into the interior fluid.

Using data from the computer simulations that produced the previous plot allowed the computation of radial intensity vectors at the shell wall. The radial intensity was calculated using the time-averaged intensity relationship of Eq. (16) and is plotted in Figs. 6 and 7 for various circumferential angles. As the main purpose of these plots is to illustrate how intensity varies with angle, the vectors are plotted so as to be normalized to the maximum value calculated in each case.

The results of Fig. 6 were produced using a source located two shell radii from the shell dipole axis, i.e., $R_s=2$. Thus the shell surface nearest the source was toward the edge of the source near field. The observation point is in the source plane $X=0$. The intensity vectors demonstrate that in the source plane, when $R_s=2$, most of the acoustic energy enters the interior cavity in localized "hot spots" close to the source, where $\theta=0$ deg.

To contrast the results of Fig. 6, the radial intensity vectors were calculated for a dipole source location of $R_s=10$. Thus, the shell surface is now totally located in the source far field. Figure 7 shows the circumferential variation in radial intensity for this case. As one can see, somewhat sur-

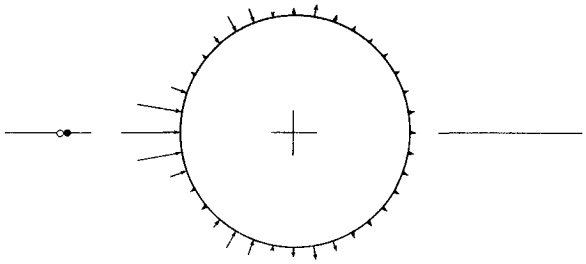

Fig. 6 Normalized radial intensity at shell wall, $X=0$, $R_s=2$, and $\Omega=0.2$ (dipole source).

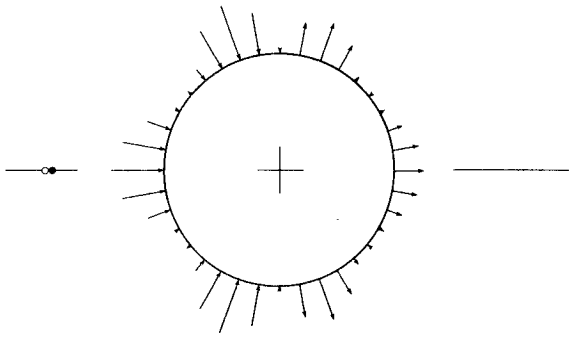

Fig. 7 Normalized radial intensity at shell wall, $X=0$, $R_s=10$, and $\Omega=0.2$ (dipole source).

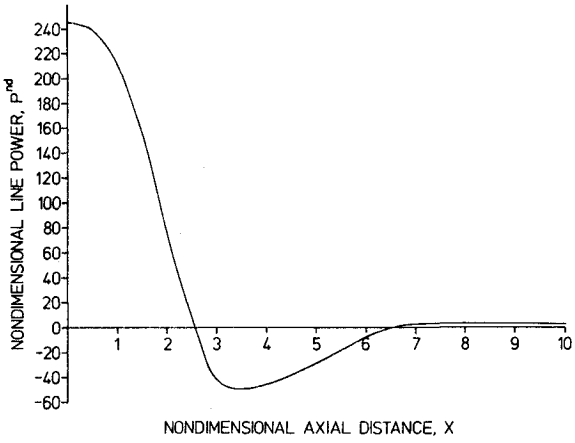

Fig. 8 Axial line power distribution, $R_s=3$ and $\Omega=0.2$ (monopole source).

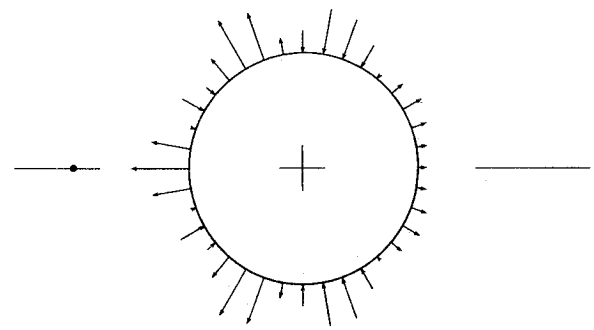

Fig. 9 Normalized radial intensity at shell wall, $X=5$, $R_s=3$, and $\Omega=0.2$ (monopole source).

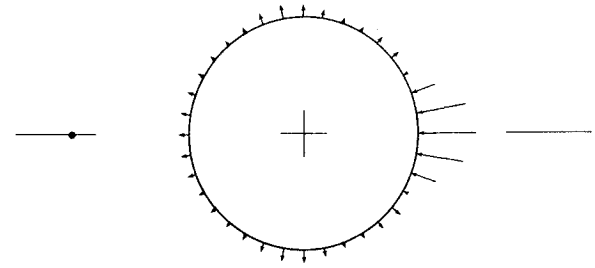

Fig. 10 Normalized radial intensity at shell wall, $X=10$, $R_s=3$, and $\Omega=0.2$ (monopole source).

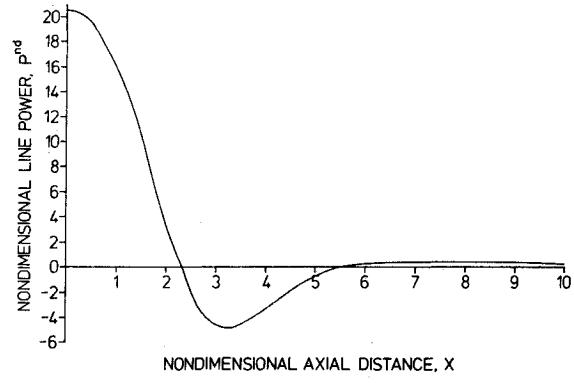

Fig. 11 Axial line power distribution, $R_s=3$ and $\Omega=0.2$ (dipole source).

prisingly, the maximum intensity occurs at $\theta=\pm 70$ deg while there is still an acoustic "hot spot" located near $\theta=0$ deg. Again, these results illustrate the importance of shell modal response interacting with the direct radiated field in determining the nature of the acoustic field transmitted to the interior cavity. In general, energy flows into the front hemisphere of the interior cavity (-90 deg$\leq\theta\leq 90$ deg) and flows out the back hemisphere (90 deg$\leq\theta\leq 270$ deg) for one source excitation and the low shell nondimensional frequencies considered here.

A few comments can be stated about the distribution of energy flux as shown in Figs. 6 and 7. From these results, and others not presented, it is clear that, as the separation distance between the shell surface and source is increased, the energy flux variation becomes relatively more uniform about the shell in the angular direction. This "spreading" of the energy flux around the shell interior is due to a combination of acoustic diffraction of the exterior source direct field and shell vibration response. Also, since the shell is elastic, it is possible that a portion of the interior radiant energy can be transmitted about the shell (i.e., in the shell material itself) through normal shell modes of vibration. In this case, the shell could subsequently reradiate this energy at various "hot spots" about the shell interior surface.

Acoustic calculations were also performed at axial locations out of the source plane. Figures 8-10 depict results of monopole radiation. Figure 8 presents nondimensional line power at different axial locations when the source is located at $R_s=3$. It is seen in Fig. 8 that most of the acoustic energy enters the shell interior in the region of $0\leq X\leq 2.5$ for one-half the infinite shell system. Thus, the acoustic energy enters the interior space in a localized area centered on the source plane and then propagates as duct modes (in a compliant tube) to locations away from the source plane. Also, note that there is a length of shell immediately after the inflow region where a significant amount of energy flows out of the interior space. This outflow of energy was thought to be due to the near field of the "shell"-type waves extending further in the axial direction than the "duct"-type acoustic waves on the interior. Because the free speed of propagation of shell waves is much faster than air, the shell is being driven at a much lower nondimensional frequency than the contained air. Thus, the shell near field decays much slower

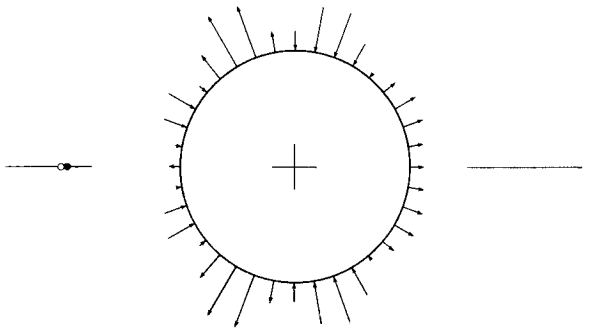

Fig. 12 Normalized radial intensity at shell wall, $X=5$, $R_s=3$, and $\Omega=0.2$ (dipole source).

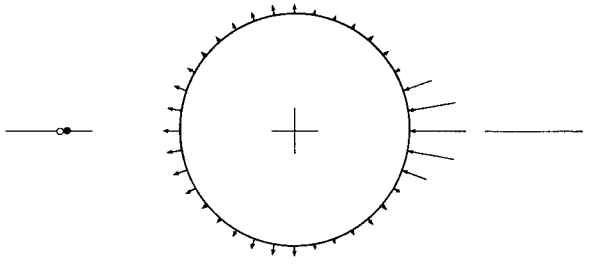

Fig. 13 Normalized radial intensity at shell wall, $X=10$, $R_s=3$, and $\Omega=0.2$ (dipole source).

than the acoustic interior near field, and the interaction of the nonorthogonal waves leads to a subsequent reradiation of sound. Similar behavior has been observed in energy distributions in vibrating fluid-filled cylinders.[5] At $X\geq 6.5$, energy again enters the interior, though the magnitude is much less than that found near the source plane.

Radial intensity vectors were calculated for two axial stations from the data used to construct Fig. 8. In Fig. 9, the circumferential variation of radial intensity for axial location $X=5$ is shown. An interesting result is that, in the plane of the source ($\theta=0$ deg), the energy flux is toward the source. This is also the maximum calculated intensity vector, and a perusal of the plot indicates that most of the energy flux is outward, consistent with the results of Fig. 8.

Figure 10 gives the radial intensity vectors calculated at an axial location corresponding to $X=10$. The monopole source is still located at $R_s=3$ so that the distance between the source and the observation plane has increased considerably compared to the previous figure. The most surprising result of Fig. 10 is that the maximum intensity vector occurs at $\theta=180$ deg, well on the backside of the hemisphere away from the source. In this region the shell is in the source far field. The net power flow is inward into the cavity.

Figures 11-13 are for configurations similar to the previous three figures except that now source directivity is introduced and studied by using a dipole source. The nondimensional acoustic line power as a function of shell axial location for a constant source location of $R_s=3$ is presented in Fig. 11. As before, this plot indicates that the monopole source is a more effective radiator than the dipole and consequently leads to greater shell response. Directivity of the source appears to have little effect on the axial distribution of line power although the region of inflow of acoustic power centered on the source plane is slightly narrowed for a dipole source. Thus, one can conclude that the near-field nature of the source dominates the distribution of acoustic energy into the interior when $R_s\approx 3$.

However, the distribution of acoustic energy shows a different behavior. In Fig. 12, the results for an axial location of $X=5$ are presented. Here, it is seen that the directionality of the source has noticeably influenced the variation in radial intensity. In contrast to Fig. 9, which depicted monopole radiation, the "hot spot" of outward intensity flow at $\theta=0$ deg is absent in Fig. 12. For this case the maximum intensity flow occurs at $\theta=\pm 60$ deg. Figure 13 demonstrates the circumferential variation in radial intensity for an axial location of $X=10$, which is well into the source far field. A comparison with Fig. 10 shows that the radial intensity distribution is little changed for the case of dipole radiation. Therefore, it appears that source directivity effects are most important in the transition region between the source near field and far field.

The results presented here by no means completely describe the interaction of simple sources with elastic cylinders. However, it is hoped that this brief discussion has led to an increased understanding of the mechanisms inherent in this important coupling problem.

Relevance of Results to Propeller Aircraft

As stated previously, the main incentive for undertaking this fundamental investigation was to learn more about how propeller noise transmits into an aircraft fuselage. Although the application of the results from this analysis to aircraft appear rather tenuous, it must be remembered that no previous work of this nature exists. Thus, the interpretation of the fundamental results in the light of real aircraft characteristics at best represents a first order of attempt. However, the authors feel that the results do shed light on an area for which little physical understanding was previously available.

Hence, on the basis that the aircraft fuselage is represented by an infinite cylinder[3] and the propeller acoustic sources are represented by dipoles (as suggested by the results of Mahan and Fuller[7]), one can draw a number of tentative conclusions about the nature of transmission of propeller noise into aircraft fuselages.

First, it appears that the near-field characteristics of propeller acoustic sources dominate the transmission mechanisms in the propeller plane ($X=0$). Directivity of the propeller acoustic source appears to play little part. Thus, the results suggest that there is a critical region in which a propeller creates high interior noise levels. Hence, there is some benefit to be obtained in terms of interior reduction by moving the propeller away from the fuselage until its acoustic source is at the edge of the near-field zone. From the results of this analysis, this distance would tentatively be one to three fuselage radii from the fuselage surface.

Second, the location of the propeller acoustic source affects the location of the interior acoustic hot spots. The area of high energy flow into the cabin is not necessarily nearest the propeller source due to the modal response of the fuselage. This has important implications for the location of passive and active noise control devices.

Third, the results suggest that most of the acoustic energy will enter the fuselage in a region around the propeller plane. Thus, any noise treatment of the fuselage need be applied only in this region. The analytical results suggest a fuselage length of the order of a fuselage diameter each side of the propeller plane.

Conclusions

An analysis has been presented in which the acoustic and structural response of an infinte cylinder shell-fluid system excited by either a single monopole or dipole source can be obtained in closed-form solution. The parameters of interior acoustic pressure, acoustic line power, and radial intensity flow into the interior space have been evaluated for differing source locations and observation points. The results obtained have been applied to the problem of transmission of propeller sound into aircraft fuselages. A number of conclusions can be stated:

1) The critical region for source location, in terms of reduction of interior sound levels, is within two shell radii of the shell wall.

2) An omnidirectional source results in higher *interior* acoustic levels than a dipole source.

3) Thus, the near-field characteristics of simple sources dominate the radiation mechanisms in the source plane.

4) Directivity of simple sources has only a slight effect on the distribution of acoustic line power.

5) Source directivity is most influential on the distribution of radial intensity in the transition region between source near field and far field (in the axial direction).

6) Diffraction and "spreading" of energy about the shell exterior are more of a factor when the shell is located in the simple source far field.

7) The interaction of acoustic sources with elastic cylinders is obviously a rather complex process. Further investigations of the nature of this brief presentation are needed to understand fully the source structure interaction problem at the heart of the aircraft interior noise transmission situation.

Acknowledgments

The authors are grateful to the National Aeronautics and Space Administration's Langley and Lewis Research Centers for their support of this research under Grant NAG1-390 and the NASA/American Society of Engineering Summer Faculty Fellowship Program.

References

[1]Metzger, F. B., "Strategies for Aircraft Interior Noise Reduction in Existing and Future Propeller Aircraft," SAE Paper 810560, 1981.

[2]Mixson, J. S. and Powell, C. A., "Review of Research on Interior Noise of Propeller Aircraft," AIAA Paper 84-2349, 1984.

[3]Fuller, C. R., "Noise Control Characteristics of Synchrophasing—An Analytical Investigation," AIAA Paper 84-2369, 1984.

[4]Junger, M. C. and Feit, D., *Sound, Structures, and Their Interaction*, MIT Press, Cambridge, MA, 1972, pp. 296-305.

[5]Fuller, C. R., "Monopole Excitation of Vibrations in an Infinite Cylinder Elastic Shell Filled with Fluid," *Journal of Sound and Vibration*, Vol. 96, No. 1, 1984, pp. 101-110.

[6]Mixson, J. S., Barton, C. K., Piersol, A. G., and Wilby, J. F., "Characteristics of Propeller Noise on Aircraft Fuselage Related to Interior Noise Transmission," AIAA Paper 79-0646, 1979.

[7]Mahan, J. R. and Fuller, C. R., "An Improved Source Model for Aircraft Interior Noise Studies," AIAA Paper 85-0787, 1985.